

UNIVERSITY OF BIRMINGHAM

University of Birmingham
Research at Birmingham

Butanol-Gasoline Blend and Exhaust Gas Recirculation, Impact on GDI Engine Emissions

Hergueta Santos-Olmo, Cruz; Bogarra Macias, Maria; Tsolakis, Athanasios; Essa, Khamis; Herreros, Jose

DOI:

[10.1016/j.fuel.2017.07.022](https://doi.org/10.1016/j.fuel.2017.07.022)

License:

Creative Commons: Attribution-NonCommercial-NoDerivs (CC BY-NC-ND)

Document Version

Peer reviewed version

Citation for published version (Harvard):

Hergueta Santos-Olmo, C, Bogarra Macias, M, Tsolakis, A, Essa, K & Herreros, J 2017, 'Butanol-Gasoline Blend and Exhaust Gas Recirculation, Impact on GDI Engine Emissions', *Fuel*, vol. 208, pp. 662-672. <https://doi.org/10.1016/j.fuel.2017.07.022>

[Link to publication on Research at Birmingham portal](#)

Publisher Rights Statement:

Published version <https://doi.org/10.1016/j.fuel.2017.07.022>

General rights

Unless a licence is specified above, all rights (including copyright and moral rights) in this document are retained by the authors and/or the copyright holders. The express permission of the copyright holder must be obtained for any use of this material other than for purposes permitted by law.

- Users may freely distribute the URL that is used to identify this publication.
- Users may download and/or print one copy of the publication from the University of Birmingham research portal for the purpose of private study or non-commercial research.
- User may use extracts from the document in line with the concept of 'fair dealing' under the Copyright, Designs and Patents Act 1988 (?)
- Users may not further distribute the material nor use it for the purposes of commercial gain.

Where a licence is displayed above, please note the terms and conditions of the licence govern your use of this document.

When citing, please reference the published version.

Take down policy

While the University of Birmingham exercises care and attention in making items available there are rare occasions when an item has been uploaded in error or has been deemed to be commercially or otherwise sensitive.

If you believe that this is the case for this document, please contact UBIRA@lists.bham.ac.uk providing details and we will remove access to the work immediately and investigate.

Butanol-Gasoline Blend and Exhaust Gas Recirculation, Impact on GDI Engine Emissions.

Hergueta C.¹, Bogarra M.¹, Tsolakis A.^{1*}, Essa K.¹, Herreros J. M.¹

¹Mechanical Engineering, University of Birmingham, B15 2TT, Birmingham, UK;

Email: a.tsolakis@bham.ac.uk

Abstract

A potential approach for addressing simultaneous reductions in toxic pollutants, greenhouse gas emissions and fuel consumption in gasoline direct injection (GDI) engines is the use of renewable alternative fuels. Furthermore, the combination of cleaner fuels with well-established technologies such as Exhaust Gas Recirculation (EGR) can reduce pollutant emissions and improve engine's efficiency.

In this research, the effect of 33% v/v of butanol in EN228 commercial gasoline containing 5% of ethanol (B33) and gasoline (B0) fuels under maximum admissible EGR rate at two steady state engine load (low and medium) conditions has been investigated. B33 reduces engine out carbonaceous emissions, while maintaining similar levels of nitrogen oxide emissions when compared to standard gasoline combustion. However, the physical and chemical properties of butanol (i.e. viscosity and heat of vaporization) showed a negative impact on carbon monoxide emissions at low load due to combustion inefficiencies. The addition of EGR showed a general reduction of gaseous emissions and particulate matter (except unburned hydrocarbons), a trend that was more significant for B33 at medium load. In addition, transmission electron microscope (TEM) analysis showed that B33 is formed by more similar primary particles than primary particles formed with gasoline fuel. From the engine point of view, EGR improved both Brake Specific Fuel Consumption (BSFC) and Brake Thermal Efficiency (BTE) for the studied fuels with respect to baseline conditions.

Keywords: GDI engine, Butanol, EGR, gaseous emissions, particulate matter, TEM

Nomenclature

aTDC	After Top Dead Centre
BSFC	Brake Specific Fuel consumption
bTDC	Before Top Dead Centre
BTE	Brake Thermal Efficiency
CAD	Crank Angle Degree
COV of IMEP	Coefficient of Variation of Indicate Mean Effective Pressure

dp₀	Primary particle diameter
ECU	Engine Control Unit
EGR	Exhaust Gas Recirculation
EVO	Exhaust Valve Opening
GDI	Gasoline Direct Injection
GNMD	Geometric Number Mean Diameter
HC	Hydrocarbons
IVO	Intake Valve Opening
MFB	Mass Fuel Burned
PAH	Polycyclic Aromatics Hydrocarbons
PM	Particulate Matter
TEM	Transmission Electron Microscopy
THC	Total Hydrocarbons
TWC	Three Ways Catalyst

26

27 **1. Introduction**

28 Gasoline Direct Injection (GDI) engines are fuel efficient and contribute to the reduction of
 29 carbon dioxide (CO₂) when compared to port fuel injection engines. The reasons are increased
 30 compression ratio by the charge cooling effect of the direct fuel injection, lower pumping losses,
 31 higher volumetric efficiency and more accurate injection control [1]. GDI engines also reduce
 32 pre-ignition and knock tendency as the compression temperatures are lower, and thus an enhancement
 33 in thermal efficiency by a reduction of heat losses can be achieved [2]. On the other hand, GDI
 34 engines have reported to increase the concentration of the Particulate Matter (PM) emissions [3, 4].
 35 The main sources of PM formation in GDI engines are identified as fuel piston wetting, injector fuel
 36 deposits and inadequate air-fuel mixing. Consequently, the diffusive combustion of rich-in-fuel areas
 37 promotes PM formation [5, 6], and also wall wetting by fuel impingement also produces an increment
 38 of unburned hydrocarbons (HCs) and carbon monoxide (CO) due to a significant grade of incomplete
 39 combustion [7, 8]. For this reason, emission standards such as Euro 6c, which includes a strict limit of
 40 6×10^{11} particles per kilometer and comes into force in September 2017 [9], are boosting the
 41 development of new technologies to reduce emissions in GDI.

42 A feasible short-to-midterm solution for addressing additional emissions reduction with a
 43 decreased in the demand of high quality fossil fuels is to use renewable bio-alcohols fuels such as

44 butanol, which is considered a second generation of renewable transportation fuel [10]. Butanol
45 provides complementary physicochemical properties to gasoline blends for decreasing regulated
46 emissions as well as improving combustion. Amongst these properties, higher octane number and
47 oxygen content extend the knock limit for advanced spark timings [11] and improve combustion
48 efficiency, respectively, leading to further CO and total hydrocarbons (THCs) reductions [3, 12].
49 Furthermore, butanol's higher latent heat of vaporization results in further cooling charge effect in
50 GDI engines, which increases the volumetric and thermal efficiency [13]. The higher latent heat of
51 vaporization combined with its lower adiabatic flame temperature can also assist in NO_x reduction
52 [14, 15]. By contrast, studies have reported an increase of NO_x with 35% butanol and advanced ST
53 [16, 17], or even insignificant differences in NO_x emission [18]. Conversely, butanol's high latent
54 heat of vaporization and viscosity can also have a negative effect on engine operability, associated
55 with engine's cold-start and ignition problems [19]. The lower energy density of bio-alcohols (22%
56 lower butanol than for gasoline) leads to a penalty in fuel consumption and, in most cases, Brake
57 Specific Fuel Consumption (BSFC) increases [20]. Butanol can also be an approach in satisfying the
58 regulated PM levels in modern engines due to its oxygen content, inhibiting particle formation and
59 promoting oxidation rates [21]. In the literature, butanol blends have been reported to reduce large
60 particles (40-60nm), while the formation of small particles (30nm) is promoted [22]. Transmission
61 Electron Microscopy (TEM) has extensively been used for the analysis of the PM size, morphology
62 and nanostructure of soot particles, as these parameters are directly related to the formation process of
63 the particles [23]. However, there are still limited studies on the morphology of butanol-gasoline fuels.
64 This information can provide a guide of the soot oxidation rate, as it depends on the aggregate surface
65 area to volume ratio. It has been estimated that the aggregate surface area to volume ratio, is inversely
66 proportional to primary particle diameter [24]. Therefore, small primary particles will lead to high
67 aggregate surface area favoring soot oxidation [25].

68 EGR is a widespread technique firstly used in diesel engines to limit thermal NO_x formation rate
69 by reducing combustion temperature [26]. However, this technology is primarily implemented in
70 GDI engines to obtain high engine efficiency and to improve fuel economy, since throttling losses can
71 be reduced at low/part load range [27]. EGR increases the overall charge mass so the volumetric

72 efficiency and the total heat capacity is relatively raised, leading to reduced pumping losses and lower
73 temperature of the in-cylinder walls [28]. EGR has also shown beneficial effects on decreasing the
74 severity of knock in GDI engines [22], enabling to advance the spark timing that improves the
75 combustion phasing and therefore, increasing the engine work output and the thermal efficiency [29].
76 However, EGR addition slows down the combustion speed, leading to prolonged combustions that
77 occurs over a greater proportion of engine cycle, thereby, worsening combustion stability [30].

78 In terms of emissions, EGR is reported to improve regulated emissions except for THC, mainly
79 due to the high EGR heat capacity that reduces the HC oxidation rate and may cause engine to misfire
80 when high EGR rates are used [29, 31]. The effect of EGR on particle emissions in GDI engines has
81 been also reported. Depending on the engine condition and EGR ratio, some authors have reported
82 that EGR addition increases the accumulation mode of particles and reduce nucleation mode
83 (medium loads) [32]. This effect was attributed to the lower in-cylinder temperature that reduced the
84 soot oxidation rate. This effect appeared to be more significant than the decreased in primary carbon
85 particles formed by thermal pyrolysis and dehydrogenation reaction of fuel vapor droplets, and thus,
86 the accumulation mode is increased. However, other authors have found the opposite effect, with
87 reduced accumulation mode and increased nucleation mode when EGR ratio was higher than 12% [22,
88 32]. It was attributed to the low in-cylinder temperature that limited the primary particle formation by
89 thermal pyrolysis and dehydrogenation. Additionally, the abruptly increased in HC, which are highly
90 related to nucleation mode, promoted further the increment of small particles and consequently, the
91 reduction in accumulation mode relatively to nucleation mode. Others have found reduction of 46%
92 and 90% in particle number (PN) and solid particle number, respectively, at high load and slightly
93 rich condition that simulate the transient engine conditions with cooled EGR [33].

94 Although, the use of alcohols for replacing gasoline in the GDI engines has been studied, there is
95 still a need to better understand the behavior and the potential benefits of butanol fuel in these engines
96 in terms of emissions reduction and combustion performance. The aim of this investigation is to
97 assess and to further the understanding on the effect of the utilization of high butanol fraction blends
98 on combustion characteristics, gaseous and particulate matter emissions in GDI engines. The
99 potential benefits of high-diluted combustion process with EGR are also investigated in conjunction

100 with the B33 fuel. Additionally, the analysis of the primary particle diameters of the PM agglomerates
101 emitted for both fuels has also been investigated through transmission electron microscopy (TEM).

102 **2. Materials and Methods**

103 An 2L air-guided, four cylinders turbocharged GDI engine manufacturer by Ford has been used
104 for this study. The engine was coupled to a 75kW AC dynamometer and inverter drive capable of
105 motoring and absorption/regeneration. The specifications are depicted in Table 1 and the schematic
106 of the engine and experimental set up is shown in Figure 1.

107

Table 1: GDI engine specifications

Engine Specifications	
Compression Ratio	10:1
Bore×Stroke	87.5× 83.1 mm
Turbocharger	Borg Warner k03
Rated Power	149kW at 6000rpm
Rated Torque	300Nm at 1750-4500rpm
Engine Management	Bosch ME 17

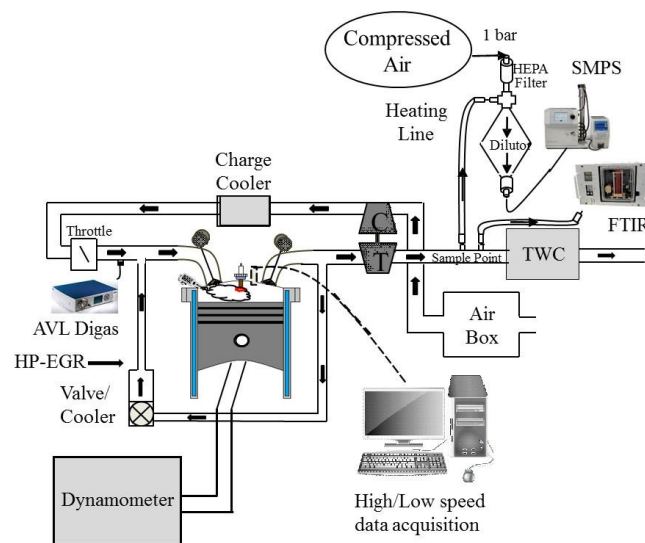
108 The engine was operated at stoichiometric conditions where the oxygen concentration was
109 controlled by a Heated Exhaust Gas Oxygen (HEGO) sensor. An AVL miniature piezo-electric
110 pressure transducer referenced to the engine cycle utilizing a Baumer 720 pulse per revolution
111 magnetic encoder was used for in-cylinder pressure measurements, considering an average of 200
112 cycles. The in-cylinder pressures were acquired using an in-house LabView application. Fuel
113 consumption was monitored with a Rheonik RM015 Coriolis fuel meter. The fuel supply temperature
114 control was provided by a fuel conditioning unit sourced from CP Engineering, and set to 28°C for the
115 test. The OEM's calibration strategy to reduce pumping losses was the utilization of valve
116 overlapping to increase the residuals. This technique is known as internal EGR, where the intake
117 valve opening (IVO) was set at 11 CAD bTDC (Crank Angle Degree before Top Dead Centre), and
118 the exhaust valve closing (EVO) is at 57 CAD aTDC (Crank Angle Degree after Top Dead Centre).
119 The engine is also equipped with high pressure external EGR system (designed and implemented by
120 the University of Birmingham). The external EGR valves were controlled using a standalone control

121 unit that requires a pulse-width modulated input signal to specify the desired valve position, provided
122 by a custom LabView application.

123 A Fourier Transform Infrared Spectroscopy (FTIR) 2100 MKS was used to measure gaseous
124 emissions (CO, CO₂, NO_x and THC). The sample was previously filtered to avoid potential damage
125 of the optical lenses by PM, and pumped via a heated line maintained at 190°C to prevent any water
126 and HC condensation. The EGR ratio was determined using eq.1 by utilising an AVL Digas 440
127 non-dispersive infrared analyzer, to measure the CO₂ concentration at the intake and exhaust.

$$EGR\ Ratio = \frac{CO_{2(intake)}}{CO_{2(exhaust)}} \cdot 100\ (%) \quad (1)$$

128 Particle size distribution measurements were carried out using a TSI scanning mobility particle
129 size composed by a series 3080 electrostatic classifiers, a 3081 Differential Mobility Analyzer and a
130 3775 Condensation Particle Counter. The sample flow and the sheath flow were set to 1 and 10 lpm
131 respectively. The distribution ranged from 7.5 to 294 nm. The sampling point was located pre-three
132 way catalyst (TWC). To prevent HCs and water condensation, the line temperature was also
133 maintained at 190 °C during the test. The samples were then diluted with air at a dilution ratio of 7-8,
134 using an ejector diluter system, fitted with a high efficiency particulate arrestance filter to
135 precondition the sample.



136 **Figure 1:** Schematic of the engine and instrumentation set up

137 A custom post-processing script was developed in Matlab to import and time-align the channels
 138 of data obtained by the multiple data acquisition sources. The Matlab function enabled a detailed
 139 combustion process analysis by means of in-cylinder pressure measurements, including heat release
 140 rate, mass fraction burned (MFB), in-cylinder pressure, total cycle indicated mean effective pressure
 141 (IMEP) and coefficient of variation (COV) of IMEP (%).

142 For the PM primary particles analysis 3.05mm TAAB Formvar coated cooper grids were used to
 143 obtain the sample. The grids were directly exposed in the engine exhaust pipe before the three-way
 144 catalyst. A JEOL 1200EX TEM LaB6 80keV operating voltage was used to obtain the micrographs
 145 for primary particle analysis.

146 3. Experimental Procedure

147 The engine was operated at two steady-state conditions from the New European Driving Cycle
 148 for a mid-size/large family vehicle with 2L engine under urban driving operation: a) 35Nm/2100rpm
 149 (low load) and b) 60Nm/2100rpm (medium load). Butanol-gasoline fuel was blended at the
 150 University of Birmingham using standard EN228 gasoline with 5% (v/v) ethanol content (B0) and
 151 pure n-butanol was used in the process. The fuel characteristics are listed in Table 2.

152 **Table 2:** Fuels properties [34-36]

Property	Gasoline	n-Butanol
Chemical formula	$C_{5.88}H_{11.06}O_{0.1}$ ^a	$C_4H_{10}O$
Density (kg/m ³)	743.9 ^a	811
Research octane number	96.8 ^a	96
Motor octane number	85.2 ^a	85
Latent heat of vaporization (kJ/kg)	350	722
Lower Heating Value LHV (kJ/kg)	42.2 ^a	33.1
Auto-ignition temperature (°C)	~300	385
Laminar flame speed (m/s)	51	58.5
Viscosity (mm ² /s) at 40°C	0.4-0.8	2.63
Adiabatic flame temperature (K)	2370	2340

153 ^a Provided by Shell

154 The blend chosen was 33% v/v (B33) of butanol in EN228 commercial gasoline containing 5%
 155 of ethanol. An IKA C200 calorimeter was used to measure the lower heating value of B33. The result

156 obtained was 40.175 MJ/kg. The test was repeated three times to ensure reproducibility and
 157 repeatability, with a maximum relative standard deviation of 0.1% between the measurements.

158 The spark timing was varied to phase the MFB50% to the one obtained for baseline gasoline for
 159 Maximum Brake Torque (8 ± 1.5 CAD aTDC timing) for comparison purposes (Table 3). Camshaft
 160 timings were fixed at short overlap setting to avoid the presence of residuals in the combustion
 161 chamber (IVO 11 CAD bTDC and EVC 8 CAD aTDC). The effect of butanol on gasoline was studied
 162 under the influence of external EGR. The conditions must satisfy the constrain of remaining COV of
 163 IMEP below 3% at maximum EGR, which is a reasonable measurement of a modern engine stable
 164 operation [35]. Prior to the test, the engine was warmed up, starting the measurement at 95 ± 0.5 °C for
 165 coolant and 95 ± 2 °C for oil. The intake air temperature was maintained at 45 ± 1 °C throughout the
 166 experiment to reduce the test-to-test variability. Otherwise, the standard Engine Control Unit (ECU)
 167 calibration settings were used such as injection timing. Confidence intervals using a 95% confidence
 168 level, which reflects the reliability and repeatability, have been calculated for gaseous emissions. All
 169 experiments were conducted on the same day for each condition to reduce the effect of day-to-day
 170 variability of the engine and emissions equipment on the results obtained.

171 **Table 3:** Engine conditions and ECU settings

			Ignition Timing	EGR (%)	Spark Timing	MFB50%
			CAD bTDC		CAD bTDC	CAD aTDC
35Nm/2100rpm	B0	Baseline	304.5	0	30.75	9.4
		Max %EGR	304.5	17	+49.5a	9.12
	B33	Baseline	304.5	0	33	9.14
		Max %EGR	304.5	17	+50.25a	8.38
60Nm/2100rpm	B0	Baseline	303.7	0	30	7.7
		Max %EGR	303.7	19	+49.5a	7.04
	B33	Baseline	303.7	0	29.7	6.9
		Max %EGR	303.7	19	+50.75a	7.9

172 + advance with respect to ECU settings

173 The study of the primary particle diameters (dp_0) for B33 and gasoline fuels where carried out at
 174 60Nm/2100rpm. For the analysis of dp_0 , manual measurements were performed, although it was only
 175 measured the apparently identifiable primary particles were measured. The recognition of the primary
 176 particles boundaries is somewhat subjective, and can lead to some fluctuations in the analysis of the
 177 results [37]. Additionally, the sample has to be large enough to ensure its log-normality distribution,

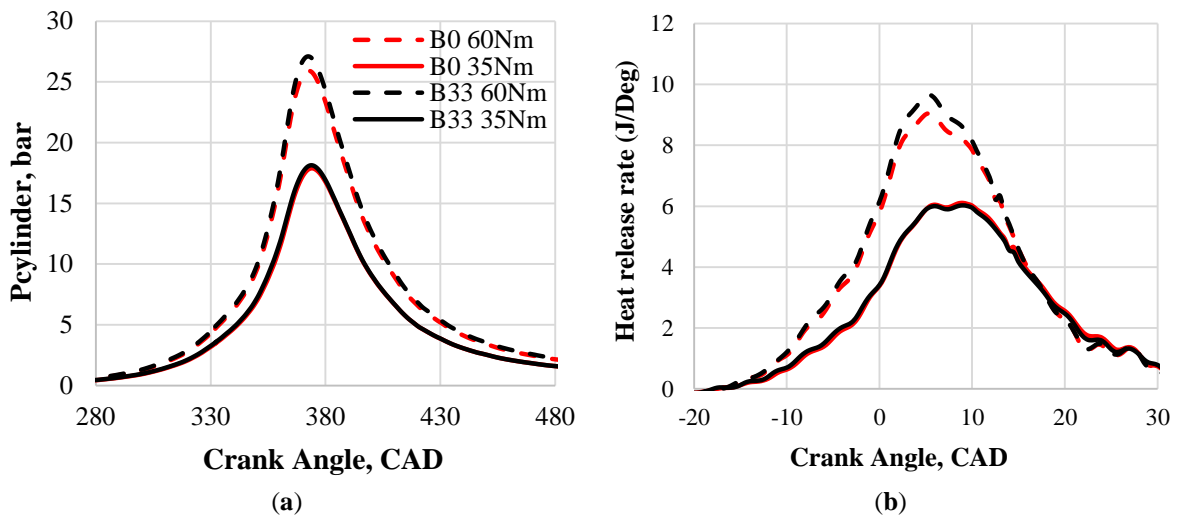
178 as Gaddam et al. [38] have discussed. At least 240 primary particles were considered per fuel, located
179 in 17 different agglomerates randomly chosen in the TEM grids. One-sample non-parametric
180 Kolmogorov Smirnov test in the IBM statistical package for social sciences software (SPSS) was
181 performance to check the log-normality.

182 **4. Results**

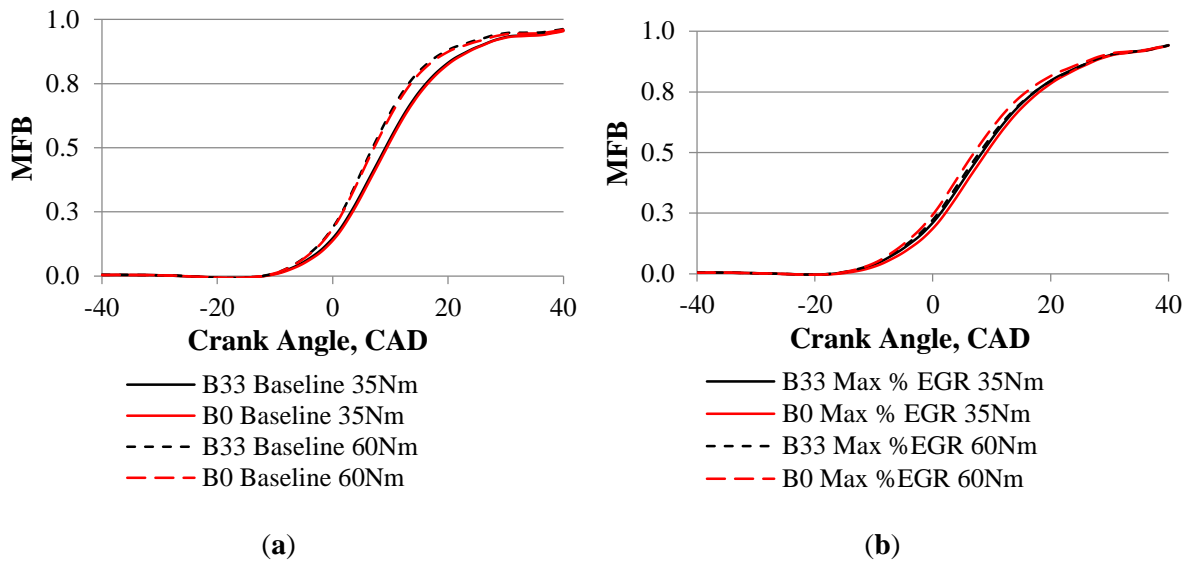
183 *4.1 Combustion studies*

184 The in-cylinder pressure and heat release rate for B33 are overlapped with respect to those
185 obtained under gasoline fueling at 35Nm (Figure 2 (a)). In addition, the MFB50% timing was kept
186 identical (Figure 3 (a)) by slightly advancing the spark timing (Table 3), so comparisons of the two
187 fuels engine-out emissions can be made based on their chemistry. It has been previously reported that
188 the higher flame speed of butanol promotes stable combustion and improves the degree of constant
189 volume heat release [34]. However, at this engine load, it seems that the fuel physical properties (i.e.
190 viscosity and enthalpy of vaporization) dominate over the faster laminar burning velocity of butanol
191 (Table 2) resulting in advanced spark timing (2.25° CAD) to achieve the same MFB50% (Figure 3 (a))
192 and slightly worse combustion stability as COV of IMEP indicates (Figure 4). It is thought that the
193 high viscosity of B33 impacts on the fuel spray atomization process, promoting more
194 in-homogeneous mixture and hence, it reduces combustion stability.

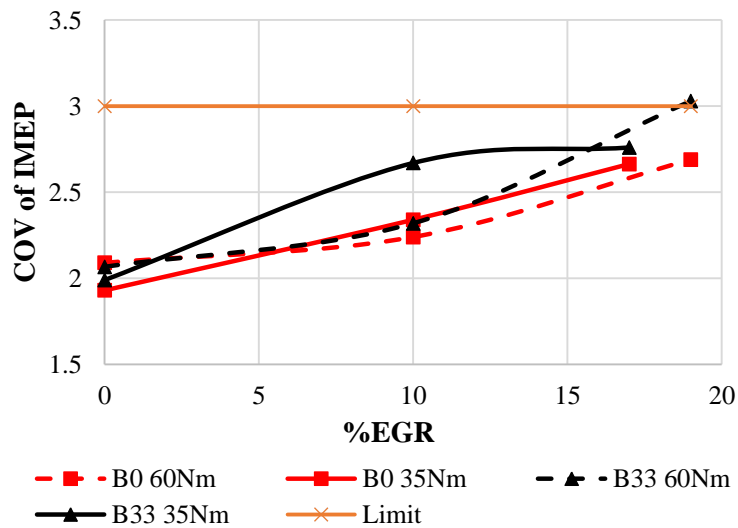
195 For the medium engine load of 60 Nm, the in-cylinder peak pressure and heat release rate of B33
196 were slightly higher compared to gasoline, which is in agreement with the results reported earlier in
197 literature [12, 22, 36, 39], at a comparable combustion phasing (Figure 3 (a)). The higher fuel spray
198 velocities, resulting from the increased engine load at 60 Nm, created a turbulent motion inside the
199 cylinder that promoted the homogeneity of the air-fuel mixture [39]. At this engine load, the higher
200 laminar burning velocity of butanol combined with an enhancement in fuel spray atomization provide
201 greater combustion quality when compared to gasoline, as observed by the lower COV of IMEP
202 (Figure 4).



203 **Figure 2:** (a) In-cylinder pressure and (b) heat release rate versus CAD for gasoline (B0) and B33 at 2100rpm



204 **Figure 3:** MFB for Gasoline and B33: (a) Baseline and (b) Max EGR at 2100rpm

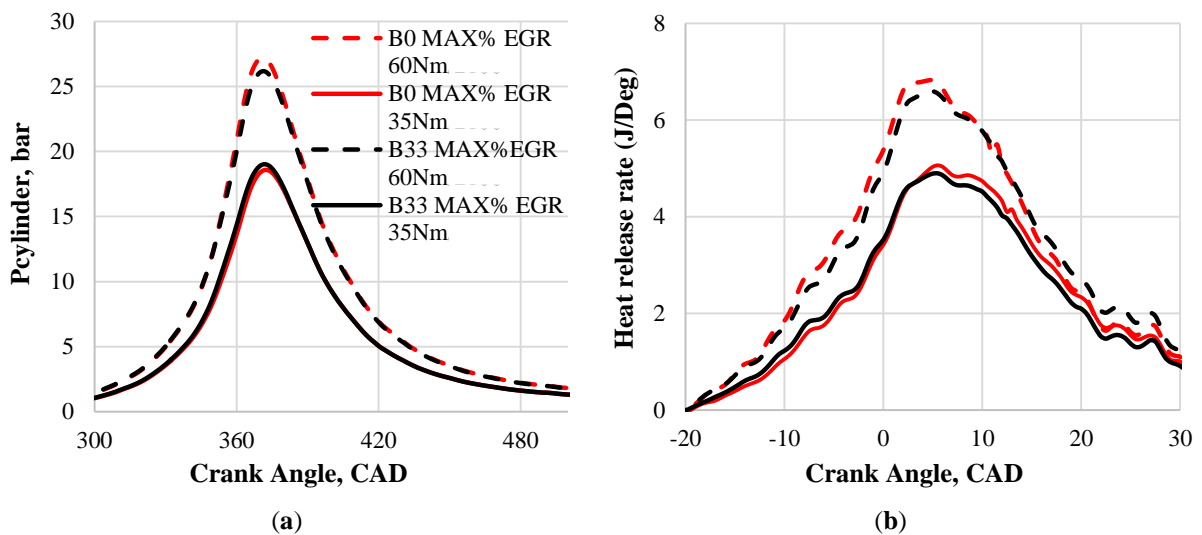


205

206

Figure 4: COV of IMEP as a function of EGR rate (%) at 2100rpm

207 The introduction of maximum applicable EGR rate (%) in B33 fueling at low and medium
208 engine load slightly reduced the in-cylinder pressure and heat release with respect to maximum EGR
209 with gasoline fuel (Figure 5). The B33 higher cooling charge capability together with the EGR
210 negatively affected the fuel vaporisation of B33, and consequently the mixture homogeneity as
211 reflected in the COV of IMEP (Figure 4), which leads to marginal peak reduction in both, the
212 in-cylinder pressure and heat release rates.

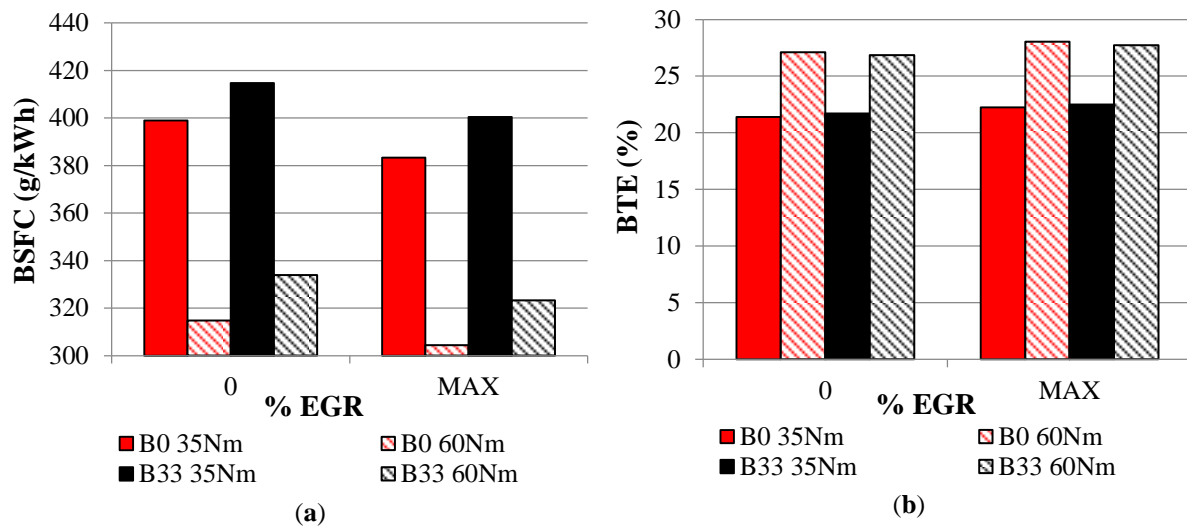


213 **Figure 5:** (a) In-cylinder pressure and b) heat release rate versus CAD for Gasoline and B33 at maximum EGR
214 and 2100rpm

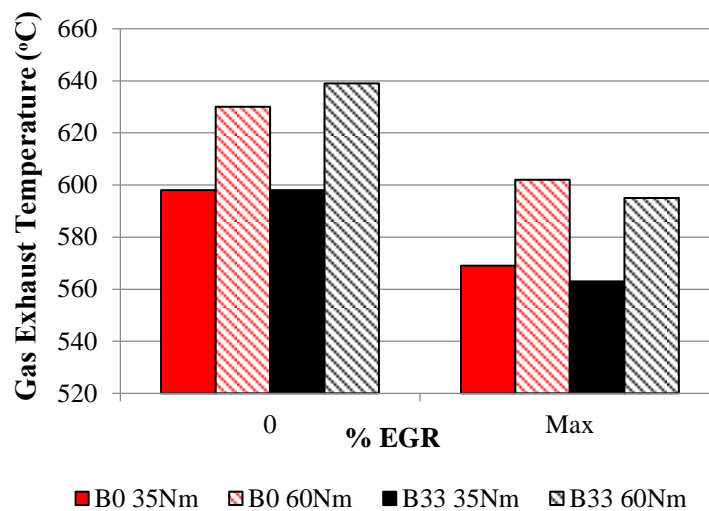
215 Figure 6 (a) shows that the EGR enhances the BSFC for both fuels, in agreement with the
216 literature [8, 32]. When EGR is used, the throttle valve must be further opened in order to maintain the
217 oxygen level at stoichiometric ratio and therefore, the pumping losses are reduced. In all cases, the
218 BSFC of B33 combustion was higher in comparison to gasoline combustion. The brake thermal
219 efficiency, which is inversely proportional to the BSFC, and considers the lower heating value of the
220 fuel blends is shown in Figure 6 (b). There are no significant differences in the indicated thermal
221 efficiency which concludes that the higher BSFC in the case of the B33 blend is due to the lower
222 energy density of butanol compare to gasoline [36].

223 As it can be observed from the reduction of the exhaust gas temperatures (Figure 7), EGR brings
224 the in-cylinder temperature down, enabling a reduction of the heat losses to the coolant and

225 surroundings, and contributing in further improvements of the brake thermal efficiency (BTE) [22,
 226 32]. Thus, EGR enhances BTE (Figure 6 (b)) for the gasoline and B33 combustion at both engine
 227 loads. Although B33 worsens the BSFC compared to gasoline, the higher heat of vaporization of B33
 228 can improve the volumetric efficiency and reduce the heat losses to the coolant and surroundings. The
 229 physicochemical properties of butanol in gasoline blend is reflected in a BTE similar than for gasoline
 230 as the differences are around 1% at both engine conditions (Figure 6 (b)).



231 **Figure 6:** a) Brake Specific Fuel Consumption BSFC and b) BTE with and without max %EGR ratio at
 232 2100rpm.



233 **Figure 7:** Exhaust gas temperature at baseline and max % EGR at 2100 rpm

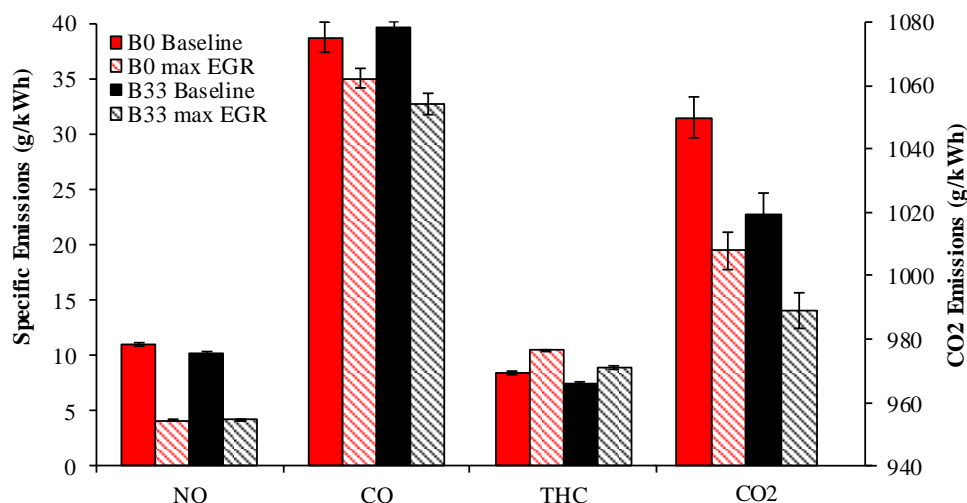
235

236 4.2 Gaseous Emissions

237 THCs and CO emissions provide a direct insight into the combustion process by contributing to
238 the evaluation of the combustion efficiency. The combustion of B33 at 35Nm resulted in slightly
239 lower THC emissions compared to gasoline (Figure 8). Although both the oxygen content of B33 and
240 its shorter carbon chain length are promoting higher oxidation rates to CO₂, the poor butanol spray
241 and mixing properties at low load inhibit this oxygen effect, increasing CO emissions [40] through
242 incomplete combustion. A significant decrease in THC and CO is noticeable at 60Nm (Figure 9) with
243 the combustion of B33 compared to gasoline. The greater combustion stability, as it can be observed
244 from the COV of IMEP and, higher combustion temperature and heat release rate may be the reasons.
245 The exhaust gas temperature of B33 at 60Nm raised by nearly 10 °C (Figure 7) with respect to
246 gasoline combustion, which is an indication of higher in-cylinder temperature for B33. This resulted
247 in a THC and CO reduction of 12.6% and 4%, respectively, as greater oxidation rates of the THC can
248 be achieved during the combustion and exhaust stages.

249 The in-cylinder pressure increases with EGR, and as a result, the fuel is forced into the piston
250 ring crevices that then is released as unburnt HC emissions during the exhaust stroke [7].
251 Furthermore, the reduction of combustion temperatures induced by the addition of EGR led to lower
252 heat release and combustion stability. This promotes lower oxidation of THC during the combustion
253 process and exhaust stroke. In addition, the lower mixing time available for fuel-air mixture due to
254 spark timing advance (a total average of 50 CAD advanced, see Table 3) can also result in poorer
255 mixture preparation, which worsens the oxidation of THC [32] for both fuels. The combustion of
256 gasoline at maximum EGR produced higher THC concentration for both engine conditions, even
257 when the stability and exhaust temperature was less favourable for B33. This effect has been reported
258 in literature for EGR rates up to 20%, THCs were found to decrease with the increasing bio-alcohol
259 content [22]. CO emissions were generally reduced with EGR addition compared to baseline
260 combustion for both fuels and engine conditions. A reason could be the reduction of liquid fuel [41]
261 due to a drop in pumping losses. Furthermore, THC oxidation is highly worsened respect to baseline
262 (Figure 8), which leads to lower CO and CO₂ emissions. CO emissions for B33 experienced a

263 significant reduction in both conditions at maximum EGR rate, accounting for 6.73% and 14.76% at
 264 35Nm and 60Nm respectively, compared to gasoline.



265

266

Figure 8: Specific gaseous emission for baseline and maximum EGR ratio at 35Nm/2100rpm for B33 and

267

B0

268

269

270

271

272

273

274

275

276

277

278

279

NOx emissions keep a clear trend at 35 Nm where a decrease of 7.65% in NOx was observed for B33; however, no significant reduction was seen at 60 Nm. At low load, the exhaust gas temperature of both fuels (Figure 7) were the same, which can indicate a narrow difference of in-cylinder temperature (source of thermal NOx formation). However, the exhaust gas temperature is not a direct measurement of the in-cylinder temperature, and no accurate prediction can be made based on an insignificant difference in exhaust gas temperature. Thus, it is thought that butanol's lower adiabatic flame temperature of B33 could reduce the local combustion temperatures compared to gasoline, being the reason for slightly NOx reduction [36, 42] at 35Nm. In addition, the marginally lower heat release rate at the end of the combustion phase could potentially reduce the NOx emissions with respect to gasoline. On the other hand, the reason for the lack of effect of B33 at 60 Nm could be the better homogenisation and stability, enabling to gain higher combustion temperature and heat release rate (Figure 2) as it can be predicted through the exhaust temperatures (Figure 7) in this case [14].

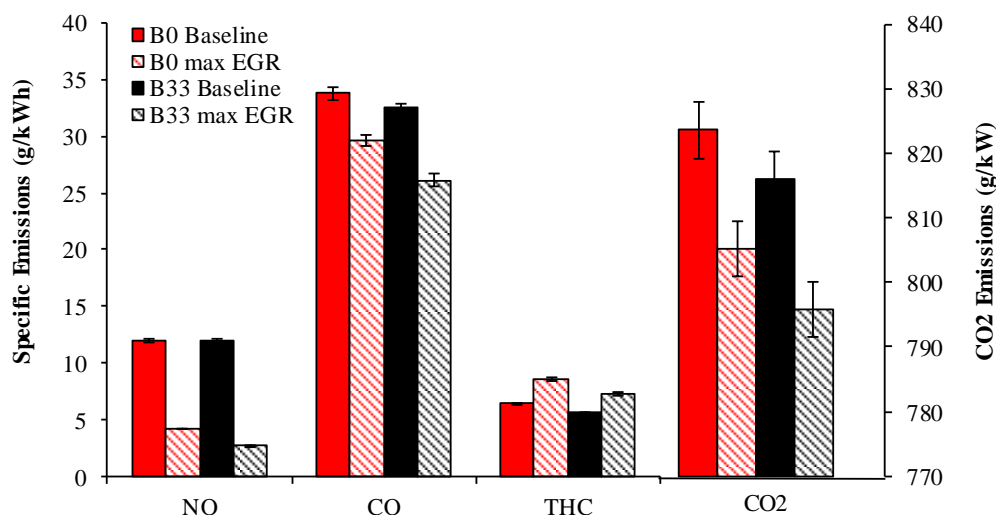
280

281

282

EGR reduces NOx emissions for both fuels. The general reason is the higher overall heat capacity in the combustion chamber limits the combustion temperature, and consequently the thermal NOx formation rate. Comparing both engine conditions and fuels at maximum EGR, there was a clear

283 reduction in NO_x of 37% at 60Nm by B33 (Figure 9), while there was not benefit in reduction of NO_x
 284 at low load (Figure 8). Assuming that the in-cylinder temperature with EGR is lower in both engine
 285 conditions for B33, which is reflected in exhaust gas temperature (Figure 7), it could be thought that
 286 NO_x emission for B33 must be lower than in the gasoline case. However, this is not observed in both
 287 engine conditions. The high viscosity of butanol together with the low injection pressure at 35Nm
 288 worsens the spray pattern and hence, the air-fuel mixture quality. Consequently, the combustion of
 289 B33 is more unstable compared to gasoline at low load. This has been reported to promote diffusive
 290 flames (precursor of NO_x emissions), and as a result, inhibiting the favourable influence of the
 291 cooling charge effect of B33 for NO_x inhibition [28].



292 **Figure 9:** Specific gaseous emissions for baseline and maximum EGR at 60Nm/2100rpm for B33 and B0

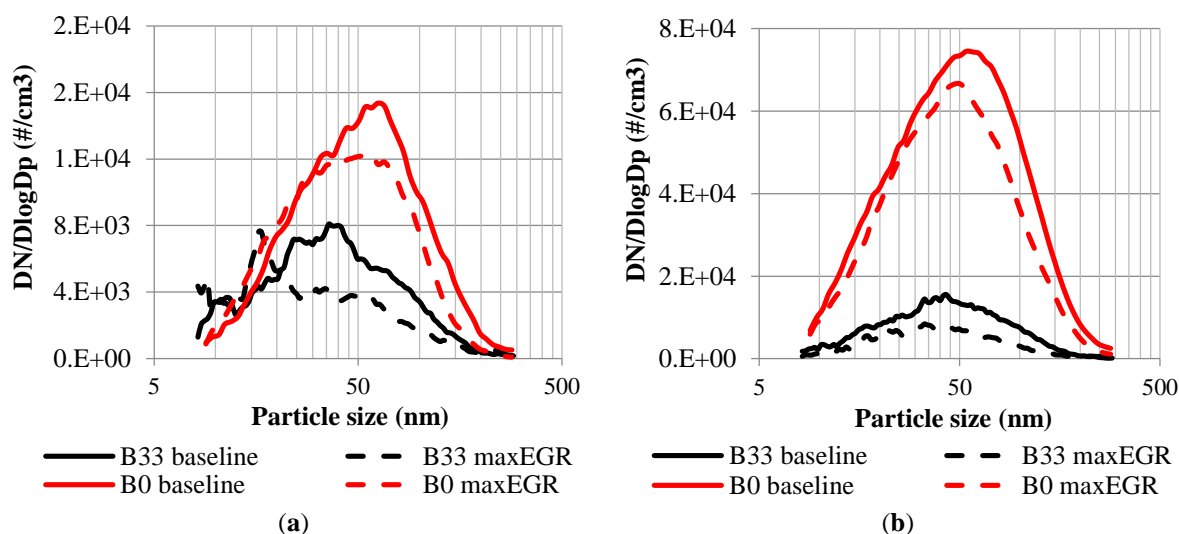
293 The combustion of B33 provided a reduction in CO₂ emissions at both loads when compared to
 294 gasoline. The decrease in CO₂ emissions with the butanol blend is due to the higher H/C and O/C ratio
 295 of B33 with respect to gasoline fuel. The CO₂ reduction is more noticeable at low load which could be
 296 attributed to a lower conversion of THC to CO₂ due to the lower combustion efficiency and lower
 297 carbon fuel content. With EGR, CO₂ experienced a reduction for both fuels. The EGR improved
 298 BSFC (Figure 6 (a)) and, consequently; a lower mass of fuel is needed to maintain the engine
 299 operation condition. In addition, the incomplete combustion of THCs, which increases its emissions,
 300 may be another cause of CO₂ reduction. At both conditions with EGR, B33 produced lower CO₂

301 emissions, which can be again ascribed to its higher H/C and O/C ratios and improved volumetric
302 efficiency due to the greater cooling charge effect with respect to baseline operation.

303 *4.3 PM Emissions*

304 Particle number size distribution from the combustion of B33 and gasoline with and without the
305 addition of EGR at maximum rates are plotted in Figure 10. At low engine load (Figure 10 (a)) during
306 baseline combustion, a unimodal particle distribution. Firstly, B33 provided a significant reduction in
307 particle concentration compared to gasoline, accounting for 60% when the peak was considered at
308 35Nm. At this engine condition, gasoline particle size distribution is displaced to larger diameters
309 with respect to B33 results. The combustion of B33 presents a peak governed by nucleation mode
310 particles with the geometric number mean diameter (GNMD) being at 30nm, exhibiting a reduction in
311 size, mass and number of particles relative to gasoline. The accumulation mode of particles has a
312 close relation to the polycyclic aromatic hydrocarbons (PAHs) as it has been reported in literature [1,
313 3, 43, 44]. Thus, the addition of butanol to the gasoline, reduces the aromatics content in the fuel
314 blend, and consequently, the number of particles with high GNMD is decreased, favoring the
315 increased number of nuclei particles [39]. In addition, the presence of oxygen as part of the alcohol
316 fuel reduces the soot formation rate and enlarges the oxidation rate during the combustion process.
317 Hence, the reductions of number and GNMD for B33 combustion decrease the number of interaction
318 between the particles, leading to lower surface growth, coagulation and aggregation processes, and
319 therefore the presence of large hydrocarbons for the formation of the accumulation mode particles
320 decreases.

321 Similar results were found at 60 Nm (Figure 10 (b)), but in this case the reduction in the peak of
322 the particle distribution was even more notable, accounting for 81% with respect to gasoline. This
323 engine condition promoted a more homogeneous air-fuel mixture for B33, which resulted in higher
324 combustion efficiency and stability (Figure 4). This enhancement in the stability was reflected in
325 higher in-cylinder pressure and heat release that indicate higher combustion temperatures shown by
326 exhaust gas temperatures in (Figure 7). Therefore, the soot and THC oxidation rate is increased,
327 enabling a greater difference between gasoline and B33 at 60Nm with respect to 35Nm.



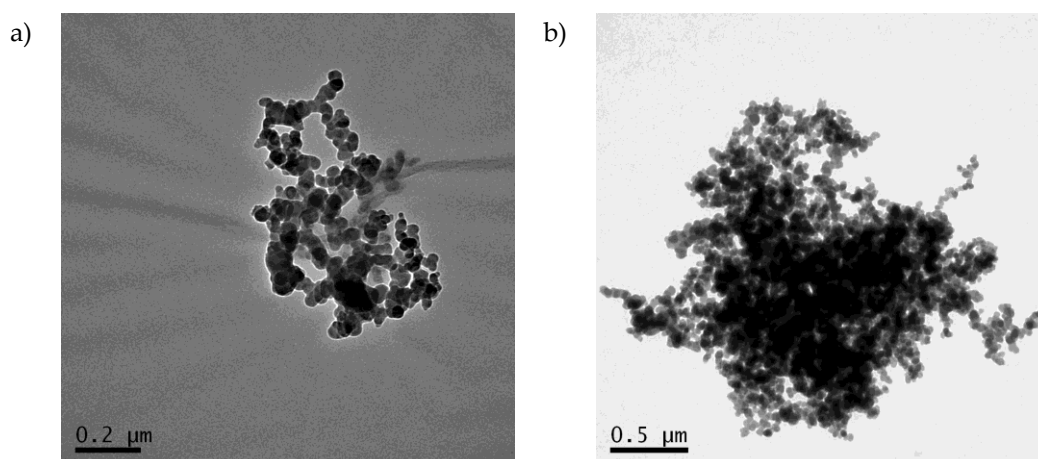
328 **Figure 10:** Effect of B33 and maximum EGR ratio on particle size distribution: a) 35Nm/2100rpm and b)
 329 60Nm/2100rpm

330 A general reduction of particle number and size was achieved under EGR conditions. A
 331 reasonable explanation for lower PM formation can be attributed to the fact that EGR generally
 332 improves engine efficiency and fuel consumption (Figure 6). Therefore, for a given engine load, less
 333 fuel is required into the cylinder compared to baseline condition, leading to proportionally less PM
 334 being formed [31]. For both fuels and conditions tested, the particle distribution peak shifts towards
 335 smaller particles sizes with the introduction of EGR, indicating a growth in proportion of finer
 336 particles in benefit of the reduction in particulate mass. The application of EGR led to a 15-20%
 337 reduction in the particle concentration peak of the distribution for both fuels and engine operating
 338 conditions. Furthermore, the temperature was reduced by EGR, and consequently primary carbon
 339 particles formed by thermal pyrolysis and dehydrogenation reaction of fuel vapor may have been
 340 decreased [45]. The consequence is that overall concentration decreased with EGR for both fuels.

341 4.4 Primary Particle Diameter (d_{p0}) Analysis

342 As reported in the previous sections, the butanol blends reduce considerably the concentration of
 343 PM independently of the engine condition and the size of the final agglomerate. Gasoline PM presents
 344 aciniform-shape formed by several nearly spherical primary particles. In this section, an analysis of
 345 the effect of butanol in the primary particle diameter (d_{p0}) has been performed at 60Nm/2100rpm, in
 346 which the PM concentration was more significantly reduced. An example of the TEM micrograph of

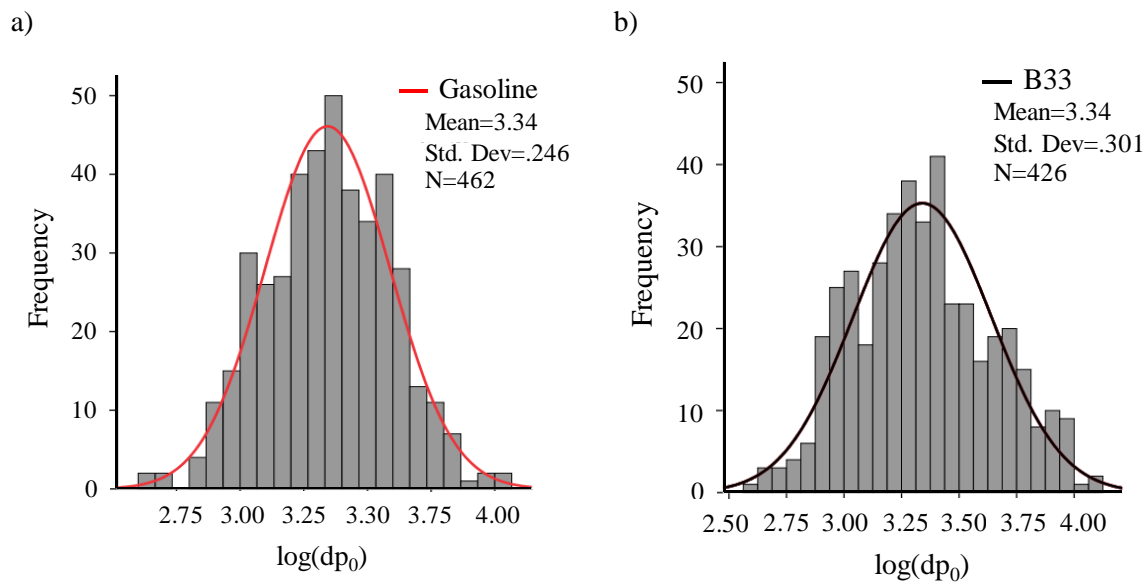
347 particles collected from the GDI engine exhaust for both fuels is shown in Figure 11. Previous studies
348 reported the presence of different types of particles in GDI engines: i) nearly-spherical HCs droplets,
349 ii) solid spherules as small as 6 nm, iii) ‘wet’ diesel-like particles and iv) ‘dry’ diesel like particles
350 [46, 47]. These types of particles were also found in B33 in this research work.



351 **Figure 11:** TEM micrographs of PM at 60Nm/2100 engine condition at standar calibration for: a) B33 and b) Gasoline

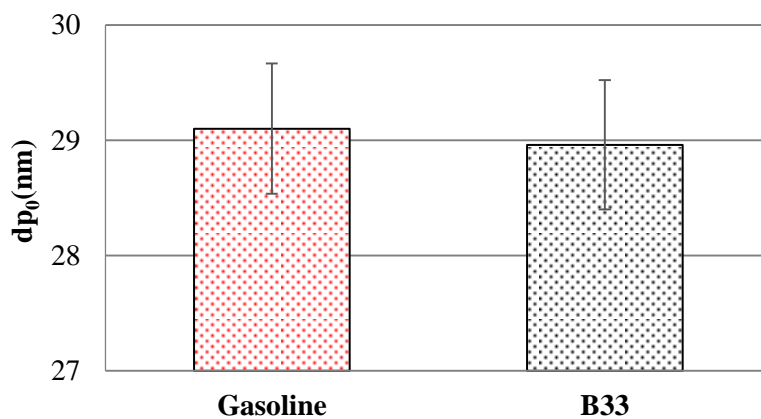
352 The log-normal primary particle size distribution for B33 and gasoline obtained by IBM
353 statistical package for social sciences (SPSS) software are shown in Figure 12. B33 particle
354 agglomerates are formed by similar mean diameter primary particles as the normal log shows. At this
355 engine condition, B33 combustion led to higher in-cylinder pressure (Figure 2, and thus, likely higher
356 in-cylinder temperature (as the exhaust temperature trends also indicates) that could increase the rate
357 of particle formation (although also the rate of oxidation), favoring the formation of primary particles
358 with higher diameters [23]. However, the presence of oxygen in B33 seems to counteract this effect,
359 maintaining the size of the formed primary particles the same as the ones recorded from the gasoline
360 combustion. The oxygen content in bio-alcohols fuels can reduce the soot formation rate and enhance
361 the formed particles oxidation rates during the combustion process, [21]. These results are similar
362 than the found for diesel bio-alcohol fuels combustion as reported in literature [48, 49], where in these
363 cases, bio-alcohols even showed slightly lower primary particles diameters due to the oxygen content.
364 Therefore, the oxygen content in B33 is likely to be helpful to limit the rate of primary particles
365 formation.

366



367 **Figure 12:** Primary particles size distributions at 60Nm/2100rpm for: a) Gasoline and b) B33

368 Additionally, the mean primary diameter and standard deviation achieved from the primary
 369 particles size distribution for B33 and gasoline are plotted in Figure 13. The average diameter for B33
 370 was in 28.96 nm while gasoline showed a diameter 29.1 nm, which was also found in our previous
 371 work for gasoline [23] . B33 formed a slightly smaller primary particle but the standard deviations
 372 overlap. Therefore, it can be concluded that the differences in primary particle diameter are negligible
 373 in this study.



374 **Figure 13:** Average primary particle diameter

375 4.4 Summary of Results

376 The effect of B33 with and without EGR are shown in Table 4, to present qualitatively the
 377 benefits of B33 in comparison to gasoline baseline combustion.

378

379

Table 4: Performance combustion of B33 combined with EGR with respect to gasoline combustion: blue + positive,

380

red - negative and - - - insignificant effect.

		BSFC	BTE	COV of IMEP	CO	THC	NOx	CO ₂	PM	
B33 35Nm/2100rpm	Baseline	--	---	-	-	+	---	++	++	
	17% EGR	-	---	---	+	---	++	++	+	dp ₀
B33 60Nm/2100rpm	Baseline	-	---	+	+++	+	---	++	+++	---
	19% EGR	-	---	--	+	---	++	++	++	

381

5. Conclusions

382

The effect of butanol 33% v/v in EN 228 commercial gasoline containing ethanol 5% v/v (B33)

383

and EGR rate on combustion characteristics and regulated emissions in a multi-cylinder GDI

384

production engine has been investigated. The influence of the butanol addition on the engine

385

combustion characteristics and emissions was dependent on engine operating (i.e. load) conditions.

386

At low engine loads, butanol's physical properties (e.g. high viscosity) are more influential on the

387

combustion performance than its chemical properties (e.g. higher flame speed). Consequently, the

388

combustion of B33 was observed to be more unstable due to the deteriorated fuel spray atomization

389

and in-homogeneous air-fuel mixture, also contributing to the marginally increased carbon monoxide

390

emissions. Conversely, butanol's shorter carbon chain and its oxygen content help to reduce the rest

391

of the emissions. As the engine load was increased, and hence the fuel injection pressure, the

392

combustion performance of B33 was improved through greater air-fuel mixture quality and

393

potentially improved spray atomization; that was reflected in an overall reduction of gaseous and

394

particulates matter emissions.

395

Transmission Electron Microscope (TEM) analysis showed that B33 did not increase the

396

primary particle diameters, even when the in-cylinder temperature was higher. This confirmed that

397

the oxygen content of butanol could limit the rate of soot formation and at the same time promote soot

398

oxidation. Therefore, in terms of the obtained soot agglomerate surface area to volume ratio, gasoline

399 and its blends with butanol are expected to have the same impact on the soot oxidation process during
400 the regeneration stages of the Gasoline Particulate Filters. It was shown that B33 was an effective fuel
401 to reduce most of the legislated emissions in both engine conditions, while maintaining engine brake
402 thermal efficiency (BTE).

403 The addition of EGR provided a general improvement of BTE and brake specific fuel
404 consumption (BSFC) for both fuels and was beneficial to B33 since greater engine-out emissions
405 reduction was achieved.

406 The research work presented here has shown that high percentages of butanol in gasoline blends
407 combined with EGR technology can be a potential solution in GDI engines for reducing legislated
408 emissions while maintaining the BTE compare to gasoline. However, it is anticipated that the
409 calibration and injection systems of the engine would have to be adapted to minimize its limited
410 performance at low loads, since the physical properties can predominate over its advantageous
411 chemical properties.

412 **Acknowledgments:** C.H.S.O. would like to thank University of Birmingham for his scholarship. M.B.M.
413 would like to thank EPSRC (Grant No: 1377213) for providing her scholarship. Innovate UK (Technology
414 Strategy Board) is acknowledged for supporting this work with the project “CO₂ Reduction through Emissions
415 Optimisation” (CREO: ref. 400176/149). The Advantage West Midlands and the European Regional
416 Development Fund as part of the Science City Research Alliance Energy Efficiency Project are also
417 acknowledged for supporting the research work.

418 **References**

- 419 1. F. Zhao, M.C. Lai, and D.L. Harrington, Automotive spark-ignited direct-injection gasoline engines.
420 *Prog. Energ. Combust.*, 1999. **25**(5): p. 437-562.
- 421 2. A.C. Alkidas, Combustion advancements in gasoline engines. *Energ. Convers. Manage.*, 2007.
422 **48**(11): p. 2751-2761.
- 423 3. G. Karavalakis, et al., The impact of ethanol and iso-butanol blends on gaseous and particulate
424 emissions from two passenger cars equipped with spray-guided and wall-guided direct injection SI
425 (spark ignition) engines. *Energy*, 2015. **82**: p. 168-179.
- 426 4. D.C. Quiros, et al., Particle effective density and mass during steady-state operation of GDI, PFI, and
427 diesel passenger cars. *J. Aerosol Sci.*, 2015. **83**: p. 39-54.

- 428 5. C. Wang, et al., Impact of fuel and injection system on particle emissions from a GDI engine. *Appl.*
429 *Energ*, 2014. **132**: p. 178-191.
- 430 6. J.E. Ketterer and W.K. Cheng, On the Nature of Particulate Emissions from DISI Engines at
431 Cold-Fast-Idle. *SAE J-Automot.Eng.*, 2014. **7**(2): p. 986-994.
- 432 7. A.O. Hasan, et al., Control of harmful hydrocarbon species in the exhaust of modern advanced GDI
433 engines. *Atmos. Environ*, 2016. **129**: p. 210-217.
- 434 8. D.A. Fennell, Exhaust Gas Fuel Reforming for Improved Gasoline Direct Injection Engine Efficiency
435 and Emissions Mechanical Engineering at University of Birmingham, Birmingham, 2014.
- 436 9. F. Steimle, et al. "Systematic Analysis and Particle Emission Reduction of Homogeneous Direct
437 Injection SI Engines", 2013-01-0248, 2013.
- 438 10. S. Heyne and S. Harvey, Assessment of the energy and economic performance of second generation
439 biofuel production processes using energy market scenarios. *Appl.Energ*, 2013. **101**: p. 203-212.
- 440 11. B. Deng, et al., The heat release analysis of bio-butanol/gasoline blends on a high speed SI (spark
441 ignition) engine. *Energy*, 2013. **60**: p. 230-241.
- 442 12. Z. Chen, et al., Impact of higher n-butanol addition on combustion and performance of GDI engine in
443 stoichiometric combustion. *Energ.Convers.Manage*, 2015. **106**: p. 385-392.
- 444 13. J.M. Bergthorson and M.J. Thomson, A review of the combustion and emissions properties of
445 advanced transportation biofuels and their impact on existing and future engines.
446 *Renew.Sust.Energ.Rev.*, 2015. **42**: p. 1393-1417.
- 447 14. R. Feng, et al., Experimental study on SI engine fuelled with butanol–gasoline blend and H₂O
448 addition. *Energ.Convers.Manage*, 2013. **74**: p. 192-200.
- 449 15. B.R. Wigg, A Study on the Emissions of Butanol Using a Spark Ignition Engine and their Reduction
450 Using Electrostatically Assisted Injection. Mechanical Engineering at University of Illinois,
451 Urbana-Campaign, 2011.
- 452 16. B. Deng, et al., The challenges and strategies of butanol application in conventional engines: The
453 sensitivity study of ignition and valve timing. *Appl.Energ*, 2013. **108**: p. 248-260.
- 454 17. M. Pechout, M. Mazac, and M. Vojtisek-Lom. "Effect of Higher Content N-Butanol Blends on
455 Combustion, Exhaust Emissions and Catalyst Performance of an Unmodified SI Vehicle Engine",
456 SAE, 2012-01-1594, 2012.
- 457 18. T. Wallner, S.A. Miers, and S. McConnell, A Comparison of Ethanol and Butanol as Oxygenates
458 Using a Direct-Injection, Spark-Ignition Engine. *J.Eng.Gas.Turb.Power*, 2009. **131**(3): p.
459 032802-032802.
- 460 19. G. Broustail, et al., Comparison of regulated and non-regulated pollutants with iso-octane/butanol and
461 iso-octane/ethanol blends in a port-fuel injection Spark-Ignition engine. *Fuel*, 2012. **94**: p. 251-261.
- 462 20. F. Catapano, et al. "Effects of Ethanol and Gasoline Blending and Dual Fueling on Engine
463 Performance and Emissions", SAE, 2015-24-2490, 2015.
- 464 21. E.J. Barrientos, et al., Particulate matter indices using fuel smoke point for vehicle emissions with
465 gasoline, ethanol blends, and butanol blends. *Combust.Flame*, 2016. **167**: p. 308-319.
- 466 22. Z. Zhang, et al., Combustion and particle number emissions of a direct injection spark ignition engine
467 operating on ethanol/gasoline and n-butanol/gasoline blends with exhaust gas recirculation. *Fuel*,
468 2014. **130**: p. 177-188.

- 469 23. M. Bogarra, et al., Impact of exhaust gas fuel reforming and exhaust gas recirculation on particulate
470 matter morphology in Gasoline Direct Injection Engine. *J. Aerosol Sci.*, 2017. **103**: p. 1-14.
- 471 24. T.L. Barone, et al., Inertial deposition of nanoparticle chain aggregates: Theory and comparison with
472 impactor data for ultrafine atmospheric aerosols. *J. Nanopart. Res.*, 2006. **8**(5): p. 669-680.
- 473 25. P. Karin, et al., Morphology and oxidation kinetics of CI engine's biodiesel particulate matters on
474 cordierite Diesel Particulate Filters using TGA. *Int. J. Automot. Techn.*, 2017. **18**(1): p. 31-40.
- 475 26. K.H. Yoo, et al. "Experimental Studies of EGR Cooler Fouling on a GDI Engine", SAE Technical
476 Paper, 2016-01-1090, 2016.
- 477 27. G. Fontana and E. Galloni, Experimental analysis of a spark-ignition engine using exhaust gas recycle
478 at WOT operation. *Appl.Energ.*, 2010. **87**(7): p. 2187-2193.
- 479 28. H. Wei, et al., Gasoline engine exhaust gas recirculation – A review. *Appl.Energ.*, 2012. **99**: p. 534-544.
- 480 29. J.M. Luján, et al., Influence of a low pressure EGR loop on a gasoline turbocharged direct injection
481 engine. *Appl.Therm.Eng.*, 2015. **89**: p. 432-443.
- 482 30. W. Zeng, M. Sjöberg, and D.L. Reuss, Combined effects of flow/spray interactions and EGR on
483 combustion variability for a stratified DISI engine. *Proc.Combust.Inst.*, 2015. **35**(3): p. 2907-2914.
- 484 31. D. Fennell, J. Herreros, and A. Tsolakis, Improving gasoline direct injection (GDI) engine efficiency
485 and emissions with hydrogen from exhaust gas fuel reforming. *Int. J. Hydrogen Energy*, 2014. **39**(10):
486 p. 5153-5162.
- 487 32. T. Lattimore, et al., Investigation of EGR Effect on Combustion and PM Emissions in a DISI Engine.
488 *Appl.Energ.*, 2016. **161**: p. 256-267.
- 489 33. M. Hedge, et al., Effect of EGR on Particle Emissions from a GDI Engine. *SAE Int. J. Engines* 2011. **4**:
490 p. 650-666.
- 491 34. C. Tornatore, et al., Optical diagnostics of the combustion process in a PFI SI boosted engine fueled
492 with butanol–gasoline blend. *Energy*, 2012. **45**(1): p. 277-287.
- 493 35. R. Scarcelli, et al. "Cycle-to-Cycle Variations in Multi-Cycle Engine RANS Simulations", SAE
494 Technical Paper, 2016-01-0593, 2016.
- 495 36. A. Irimescu, et al., Combustion process investigations in an optically accessible DISI engine fuelled
496 with n-butanol during part load operation. *Renew.Energ.*, 2015. **77**: p. 363-376.
- 497 37. K. Kondo, et al. "Uncertainty in Sampling and TEM Analysis of Soot Particles in Diesel Spray Flame",
498 SAE Technical Paper, 2013-01-0908, 2013.
- 499 38. C.K. Gaddam and R.L. Vander Wal, Physical and chemical characterization of SIDI engine
500 particulates. *Comb. Flame*, 2013. **160**(11): p. 2517-2528.
- 501 39. R. Daniel, et al., Ignition timing sensitivities of oxygenated biofuels compared to gasoline in a
502 direct-injection SI engine. *Fuel*, 2012. **99**: p. 72-82.
- 503 40. E. Galloni, et al., Performance analyses of a spark-ignition engine firing with gasoline–butanol blends
504 at partial load operation. *Energ.Convers.Manage.*, 2016. **110**: p. 319-326.
- 505 41. M. Bogarra, et al., Study of particulate matter and gaseous emissions in gasoline direct injection engine
506 using on-board exhaust gas fuel reforming. *Appl. Energ.*, 2016. **180**: p. 245-255.
- 507 42. S.S. Merola, et al., Optical diagnostics of early flame development in a DISI (direct injection spark
508 ignition) engine fueled with n-butanol and gasoline. *Energy*, 2016. **108**: p. 50-62.
- 509 43. X. Gu, et al., Emission characteristics of a spark-ignition engine fuelled with gasoline-n-butanol
510 blends in combination with EGR. *Fuel*, 2012. **93**: p. 611-617.

- 511 44. J.M. Storey, et al., Novel Characterization of GDI Engine Exhaust for Gasoline and Mid-Level
512 Gasoline-Alcohol Blends. *SAE Int. J. Fuels Lubr*, 2014. **7**: p. 571-579.
- 513 45. T. Alger, et al., The Role of EGR in PM Emissions from Gasoline Engines. *SAE Int. J. Fuels Lubr*,
514 2010. **3**: p. 85-98.
- 515 46. P. Karjalainen, et al., Exhaust particles of modern gasoline vehicles: A laboratory and an on-road
516 study. *Atmos. Environ.*, 2014. **97**: p. 262-270.
- 517 47. T.L. Barone, et al., An analysis of direct-injection spark-ignition (DISI) soot morphology. *Atmos.*
518 *Environ.*, 2012. **49**: p. 268-274.
- 519 48. M.A. Fayad, et al., Manipulating modern diesel engine particulate emission characteristics through
520 butanol fuel blending and fuel injection strategies for efficient diesel oxidation catalysts. *Appl. Energ.*,
521 2017. **190**: p. 490-500.
- 522 49. H. Yang, et al., Experimental investigation into the oxidation reactivity and nanostructure of
523 particulate matter from diesel engine fuelled with diesel/polyoxymethylene dimethyl ethers blends.
524 *Sci. Rep.*, 2016. **6**: p. 37611.

525 |